Earthq Eng & Eng Vib (2020) 19: 561-571 **DOI**: https://doi.org/10.1007/s11803-020-0580-z

Seismic resilience of retrofitted RC buildings

Ghazanfar Ali Anwar† and You Dong‡

Department of Civil and Environmental Engineering, The Hong Kong Polytechnic University, Hong Kong, China

Abstract: Existing buildings can be at a greater seismic risk due to non-conformance to current design codes and may require structural retrofitting to improve building performance. The performance of buildings is measured in terms of immediate consequences due to direct damage, but the continuing impacts related to recovery are not considered in seismic retrofit assessment. This paper introduces a framework of retrofit selection based on the seismic resilience of deficient buildings retrofitted with the conventional mitigation approaches. The assembly-based methodology is considered for the seismic resilience assessment by compiling a nonlinear numerical model and a building performance model. The collapse fragility is developed from the capacity curve, and the resulting social, economic, and environmental consequences are determined. The seismic resilience of a building is assessed by developing a downtime assessment methodology incorporating sequence of repairs, impeding factors, and utility availability. Five functionality states are developed for the building functionality given investigated time interval, and a functionality curve for each retrofit is determined. It is concluded that seismic resilience can be used as a performance indicator to assess the continuing impacts of a hazard for the retrofit selection.

Keywords: resilience; reinforced-concrete; performance-based; seismic retrofit; non-ductile

1 Introduction

Seismic hazard is a low probability high consequence event, which until 1961 was considered in the seismic provisions of Uniform Building Code (UBC) as a single lateral load on a building equivalent to 7.5% of the buildings weight (10% in the case of poor soil conditions). It was not until 1960 when seismic design provisions were made mandatory for the communities in USA adopting UBC codes. Two major earthquakes, Alaska 1964, and San Fernando 1971, revealed poor structural performance of buildings which resulted in developing new seismic design procedures (Beavers, 2002). Improving seismic design codes is an ongoing process, and it is not until recently that the seismic design codes are being implemented in low-to-moderate seismicity regions (Mwafy and Elkholy, 2017). The existing building infrastructure around the world is therefore at risk of poor performance in an earthquake event due to inadequate structural detailing and inefficient seismic design provisions implemented during the design and construction of these buildings (Gautam and Chaulagain, 2016). The seismic loss can be significant for the deficient existing buildings, particularly in low-to-medium seismicity regions where the seismic codes have not been adopted. This highlights the importance of improving the performance of existing deficient structures to reduce seismic consequences and increase resilience.

Repair, rehabilitation, and retrofitting is used to improve the performance of existing buildings. Recently, it has become an important construction activity, considering that the amount of money spent globally on repair and rehabilitation of existing structures is higher than new constructions (Ma *et al*., 2017). The retrofitting techniques include adding lateral force-resisting systems or upgrading the existing elements for structural performance improvement (Zheng *et al*., 2019). The upgrading of existing elements can be implemented by either reducing the demands on a lateral force-resisting or improving the capacity, achieved by modifying strength, stiffness, ductility properties or through any of these combinations (Thermou and Elnashai, 2006). Ductility depends on the detailing of structural components; therefore, its retrofitting would require improving beam-column joints and rebar reinforcements, which can be disruptive and expensive. Hence this type of retrofitting is rarely used in the low-to-medium seismicity region (Calvi, 2013). A more desirable approach for ductility related retrofitting is to reduce the demands on the structure by modifying or replacing lateral force resisting members. This study is related to improving the strength and stiffness of existing lateral force resisting members

Correspondence to: You Dong, Department of Civil and Environmental Engineering, The Hong Kong Polytechnic University, Hung Hom, Kowloon, Hong Kong, China
E-mail: you.dong@polyu.edu.hk
†PhD; ‡Assistant Professor

Supported by: Chinese National Engineering Research Centre (CNERC) for Steel Construction (Hong Kong Branch) at the Hong Kong Polytechnic University under Project No. P0013864; Programme Code: BBV9)
Received April 6, 2020; **Accepted** June 5, 2020

by using Reinforced Concrete Jacketing (RCJ), Steel Jacketing (SJ), and Fiber-Reinforced-Polymer wrapping around columns, which is a commonly utilized approach (Billah and Alam, 2014).

Performance-based assessment is used for the seismic upgrading of existing buildings. Performance is expressed in terms of discrete performance levels defined as immediate occupancy, life safety, and collapse prevention. The performance levels are correlated with social, economic and downtime losses, but these correlations are observation based or empirical in nature, and are site specific (Whitman *et al*., 1997). This approach to risk reduction requires threshold limit state values which cannot be precisely determined for various type of buildings, since they depend on several factors, such as structural configurations, design criteria, importance factors, level of detailing, among others (Qian and Dong, 2020). The recovery time of a building, which is a key input in the seismic resilience assessment, is also related to building performance levels, which are mostly presented in crude terms (e.g., the most widely used HAZUS risk-assessment platform assumes the building to achieve full functionality within one year, irrespective of the amount of damage and hazard scenario). Numerous studies have adopted a performance-based seismic assessment approach for risk and resilience evaluation (Dong and Frangopol, 2015; Zheng *et al*., 2018; Li *et al*., 2020a; Kilanitis and Sextos, 2019; Giouvanidis and Dong, 2020; Li *et al*., 2020b), also linking to seismic sustainability (Rodriguez-Nikl, 2015; Bocchini *et al*., 2013; Dong *et al*., 2014). A component-level approach incorporating seismic loss, sustainability and resilience has also been investigated by many researchers (Dong and Frangopol, 2016; Hashemi *et al*., 2019; Anwar *et al*., 2020; Asadi *et al*., 2019). Tirca *et al*. (2016) investigated improvement in seismic resilience through local modifications of the components of office buildings. Incremental Dynamic Analysis (IDA) was used to develop damage fragilities, and functionality curves developed by Cimellaro *et al*. (2010) were used to evaluate seismic resilience. Guo *et al*. (2017) studied seismic resilience of a frame building retrofitted with self-centering walls with friction devices. The performance of a building was compared through engineering demand parameters (EDPs), but a quantification framework for seismic resilience was not considered. Similar studies can be found in the literature for the seismic resilience improvements considering seismic retrofit (Pekcan *et al*., 2014; Vona *et al*., 2018; Khanmohammadi *et al*., 2018; Rousakis, 2018; Anelli *et al*., 2019), but none utilizes a performance-based quantification framework of resilience assessment. Molina Hutt *et al*. (2016) proposes a seismic loss and downtime assessment approach for increasing seismic resilience for tall buildings by utilizing IDA, which employs series of time history analyses with increasing intensity measure levels, and which can be computationally expensive, particularly for complex structural models, high-rise buildings, and in cases where buildings have to be analyzed several times. According to the authors' best knowledge, seismic resilience assessment of deficient reinforced concrete buildings retrofitted with conventional mitigation approaches has not been studied, especially through assembly-based quantification of downtime. Additionally, the risk assessment indicators only consider the robustness of a structure, while the resilience indicator also considers the recovery of a building. In this paper, retrofit selection is investigated based on the seismic resilience indicator.

In this paper a performance-based seismic resilience assessment framework is presented applied to a deficient reinforced concrete building. The increase in seismic resilience is investigated by applying three conventional structural mitigation approaches commonly utilized for the structural retrofit of a building. The methodology considers a component-level approach, which requires assembling a fragility and consequence functions in building performance model. The proposed assembly-based component-level approach considers the collapse fragility, determined from pushover analysis, hence bypassing computationally expensive time history analyses. Social, economic, and environmental consequences are assessed in terms of casualties, monetary loss, and equivalent carbon emissions. The seismic resilience for retrofit alternatives are assessed by developing a downtime assessment methodology incorporating sequence of repairs, impeding factors, and utility availability. The key contribution of this paper includes the development of collapse fragilities for conventional retrofit alternatives utilizing computationally efficient pushover analysis, the development of a framework for social, economic and environmental consequence assessment for considered retrofit alternatives, and retrofit selection based on seismic resilience taking into account the robustness and recovery of a building. The performance-based seismic resilience assessment methodology is presented in section 2, and an illustrative example is presented in section 3. Final section presents the conclusion of the paper.

2 Methodology

The framework begins by selecting a building and retrofit methods used for investigating and enhancing seismic resilience. The first step is to develop the nonlinear models for the reference un-retrofitted and the retrofitted buildings. The nonlinear model should be able to effectively capture the steel yielding, concrete crushing, strength, and stiffness degradation. The capacity curve representing base shear given lateral displacement can then be developed from the nonlinear static analysis procedure and is used to estimate the deficiencies in the lateral force resisting system. The capacity curves are developed by applying a series of lateral loads with increasing magnitude and recording

the lateral displacements. Increasing the lateral loads in each iteration will eventually cause elements to start to yield, and as a result of each yielding of structural members, the redistribution of loads will take place (Su *et al*., 2019). The model is revised in each iteration by adjusting the member yielding, strength and stiffness degradation, and the process continues till the yield pattern and strength and stiffness degradation for the whole structure is identified. The maximum base shear and the lateral displacements are identified and compared with the design loads and a strength factor is determined. If the strength factor is greater than one or within the desirable limits of the codes, the structure is considered safe; otherwise structural retrofitting is required. The capacity curves are developed for the retrofitted models using the same procedure (i.e., pushover analysis). If the strength factors are not desirable, then the retrofit techniques are revised and the process is repeated to achieve the desirable preliminary performance. The methodology is presented in a flowchart as shown in Fig. 1.

2.1 Developing collapse fragilities from pushover

If the retrofit techniques satisfy the preliminary strength and stiffness requirements, the next step is to develop the collapse fragilities and building performance model. Vamvatsikos and Allin Cornell (2006) investigated a series of single-degree-of-freedom systems with a wide range of time periods through incremental dynamic analysis. The resulting hysteresis loops were converted to backbone curves ranging from simple bilinear to quadrilinear, comprising an elastic, hardening, softening, and a residual plateau segment that ends at a zero-strength. The relationship between the characteristic segments of IDA curves were linked to the backbone curves of many systems, suggesting that nonlinear static analysis procedure (i.e., pushover analysis) can be used to estimate nonlinear dynamic response. In this paper, the pushover analysis is used to estimate nonlinear IDA results by utilizing the static pushover to incremental dynamic analysis (SPO2IDA) tool. FEMA (2012) recommends that this tool can be used to develop collapse fragilities for low-rise buildings dominated by the fundamental mode of vibration. This method can bypass the computationally expensive part of the methodology and can rapidly generate the collapse fragility. Following are the steps to develop collapse fragility using the SPO2IDA tool.

1. Develop a suitable nonlinear mathematical model of a structure for the pushover analysis.
2. Perform a nonlinear static analysis procedure to develop capacity curve in the principle building direction.
3. Approximate the capacity curve into quadrilinear curve by identifying four control points each indicating the endpoint and the start point of the four defined segments.
4. Execute the SPO2IDA tool and input the control points and relevant information (e.g., building weight, building height, fundamental time period etc.), and extract the median collapse capacity.
5. Construct the collapse fragility using lognormal cumulative distribution function with a dispersion of 0.6.

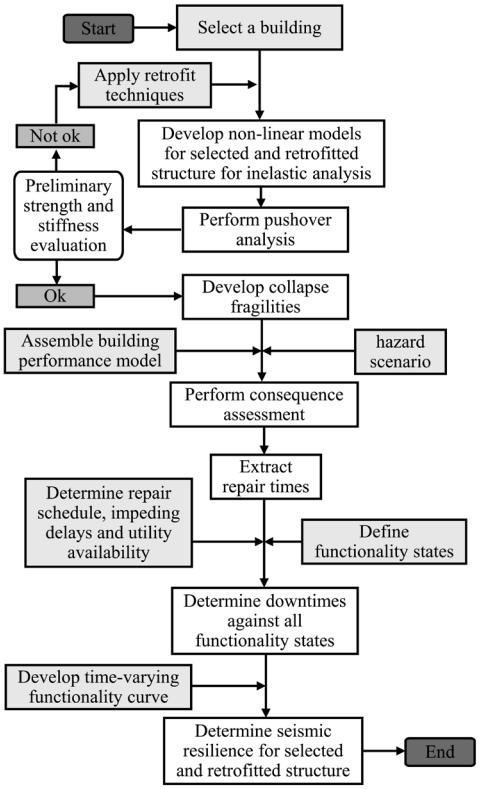

Fig. 1 The methodology for assessing seismic resilience using nonlinear static procedure

2.2 Consequence assessment

The collapse fragility analysis provides information on the probability of collapse given an intensity measure. It is more interesting for decision makers to obtain information that is more meaningful (e.g., economic loss in terms of dollars, casualties in terms of numbers, equivalent carbon emissions etc.). In the consequence assessment, collapse fragility and the probability of damage to components of a building are converted to social, economic, and environmental consequences (Dong *et al*., 2016; Wang *et al*., 2018). For that purpose, a building performance model is assembled, comprising fragility functions and consequence functions for damageable structural and non-structural components. Fragility functions determine the probability of exceeding given damage states for each damageable component. Consequence functions use the probabilities of components being in different damage states, and determine the social, economic, or environmental consequences. The following steps can determine

economic and environmental consequences given a hazard scenario.

1. Define a hazard scenario against which consequences are to be determined

2. Evaluate EDPs from the developed nonlinear mathematical model.

3. Determine probability of exceeding different damage states for all the damageable components.

4. Utilize the probability of exceeding different damage states for all the damageable components, and the collapse fragility to determine consequences using total probability theorem.

The social consequences (i.e., injuries, fatalities) can be determined as

$$S_{m|\mathrm{IM}} = \varnothing_{\mathrm{C}} T_{\mathrm{rand}} f\left(p \mid T_{\mathrm{rand}}\right) p_{\mathrm{T}} p_{\mathrm{R}} p_{\mathrm{C|IM}} \tag{1}$$

where $S_{m|\mathrm{IM}}$ is the social metric of seismic sustainability; $\varnothing_{\mathrm{C}}$ is the casualty function, which depends on the type of construction and can be determined using historical casualties from past earthquakes; T_{rand} is the randomly generated time of the day and day of the week for a particular realization; $f\left(p \mid T_{\mathrm{rand}}\right)$ is the time-dependent population model; p_{T} is the total population of a building; $p_{\mathrm{C|IM}}$ is the probability of collapse of a building given IM; and p_{R} is the population at risk depending upon the failure mode of a building.

The economic and environmental consequences can be determined as

$$C_{L_{\mathrm{T|IM}}} = \sum_{\mathrm{DS}} \int_0^{\infty} C_{L_{\mathrm{R|DS}}} p_{\mathrm{DS|EDP}} f_{\mathrm{EDP|IM}} \mathrm{dEDP} \cdot \left(1 - p_{\mathrm{C|IM}}\right) + C_{L_{\mathrm{C|C}}} \cdot p_{\mathrm{C|IM}} \tag{2}$$

where $C_{L_{\mathrm{T|IM}}}$ is the total consequence given IM; $C_{L_{\mathrm{C|C}}}$ is the consequence given probability of collapse; $p_{\mathrm{C|IM}}$ $C_{L_{R|\mathrm{DS}}}$ is the random value of a consequence loss function of a component for a given damage state; $p_{\mathrm{DS|EDP}}$ is the probability of damage state given EDP; and $f_{\mathrm{EDP|IM}}$ is the probability density function of EDP given IM.

2.3 Seismic resilience assessment

Seismic resilience is the ability of a structure to absorb damage without suffering collapse and to recover from the earthquake hazard efficiently. The building with greater seismic resilience would have less damage in an immediate aftermath of an earthquake and would recover faster. Functionality of a building after an earthquake and its recovery can be used as a performance indicator for assessing seismic resilience. The functionality curve provides the functionality state given the investigated time interval and its recovery to full functionality after a hazard event. Seismic resilience can be mathematically evaluated by integrating the functionality curve over time as shown in Eq. (3)

$$R = \int_0^{T_{\mathrm{R}}} \frac{Q(t)\mathrm{d}t}{T_{\mathrm{R}}} \tag{3}$$

where R is the resilience metric, $Q(t)$ is the functionality, and T_{R} is the investigated time interval after an earthquake.

In this paper five functionality states are developed depending upon the structural and non-structural damage and utility availability. The mapping of the functional states and the recovery to full functionality is presented in a flowchart shown in Fig. 2. Five functionality states are represented mathematically by a designated weighting factor. Full-functionality (FF) is assigning a weighting factor of 1, and the Restricted-entry (RE) is given a weighting factor of 0.2. The remaining functionality states are assigned weighting factors between 0.2 and 1 with an increment of 0.2. After an earthquake event, the process starts with the inspection of a building, which is performed by a professional building inspector. In this paper the structural and non-structural damage is computed using fragility functions to quantify the extent of damage to the building. Depending on the extent of damage and the information about the utility availability, the initial functional state of a building can be determined. For example, if the building has experienced moderate to extensive structural damage, the building is tagged in the Restricted-entry (RE) functional state (i.e., the occupants are not allowed to enter the premises before the necessary repairs). The logical sequence of repair is designed in the next step to bring the building functionality to pre-hazard state. Before the building repairs, additional delays, called impeding delays, will occur due to financing, engineering reviews, permitting, contractor mobilization and sometimes long lead times.

The building is tagged as Restricted-entry (RE) if it suffers moderate to extensive structural damage, and if the building only suffers non-structural damage, then the building is in Restricted-use (RU) functional state. The building will be recovered to full functionality after the impeding delays, necessary non-structural repairs, and availability of all the utilities. If minor or no damage is observed, then, depending upon the availability of utilities, a building is assigned as one of the remaining three functional states. If no utility is available, the building is in Re-occupancy (RO) functional state (i.e., the building space can be occupied for shelter purposes but cannot be utilized for its intended purpose). If only critical utilities are available (i.e., electricity and water), then the building is Baseline-functional (BF), and the building will achieve Full-functionality (FF) after the availability of all the utilities.

The repair time required for the repair of each damaged structural and non-structural component can be determined from Eq. (2). The downtime for each functional state can be determined by considering the

repair schedule (i.e., sequence of repairs determined from the repair times of all the damageable components), impeding delays (i.e., financing, engineering review and permitting, contractor mobilization and long lead times) and the utility availability. The impeding delays and the utility availability are considered in this paper through the lognormal distribution functioned developed by Almufti and Willford (2013) in the REDi Rating System (Resilience-based Earthquake Design Initiative for the Next Generation of Building). The functionality curve can be developed after determining the downtime for each functional state, and the seismic resilience can be evaluated.

3 Illustrative example

The non-ductile reinforced concrete building selected for this illustrative purpose is a two-story intermediate moment-resisting frame building with a total height of 8.5 m. The residential building is designed according to the building codes implemented at the time of its design and construction, which largely ignored seismic provisions, and in which only wind loads are considered in the design of a building against the lateral loads. The concrete strength of 20 Mpa and a mild steel with yield strength of 240 MPa is used for the design, resulting in large cross-sections, increased weight, and stiffness. Three retrofitting techniques, namely, Reinforced Concrete Jacketing (RCJ), Steel Jacketing (SJ), and Fiber Reinforced Polymer (FRPs) overlays are considered for improving performance of a non-ductile building. The considered seismic retrofit techniques require modifying the existing lateral force-resisting components (i.e., column in the considered example). The enhancement of the cross sections follow FEMA-547 (2006) and ASCE-41-13 (2013) recommendations, which explicitly highlight the detailing, construction practices and the seismic evaluation of existing buildings. The layout and the design details of a building are shown in Fig. 3.

Ten fiber-based nonlinear models are developed, one for the reference un-retrofitted structure and nine models for the retrofitted structures (i.e., three retrofit models for each retrofit technique). The numerical models are developed in an open source nonlinear analysis platform ZUES-NL (Jeong and Elnashai, 2005). The built-in nonlinear material models are used to represent concrete and steel behavior. The nonlinear concrete material model with crushing strain of 0.02 and a confinement factor of 1.05 is used depending upon the reinforcement details. A bilinear elasto-plastic model with kinematic strain hardening is used for the steel material modeling. The material and geometric nonlinearities, P-delta effects and large displacements are considered. The models for the reinforced concrete jacketing, steel jacketing, and FRP overlays are represented by modeling sections of the columns into reinforcing steel, confined, and unconfined concrete regions. The element cross sections are divided into number of fibers to effectively monitor the stresses and strains of different sections of elements. A uniaxial constant confinement concrete model is utilized for the reinforced concrete jacketing, a bilinear steel model with constant strain hardening is utilized for the steel jacketing, and a uniaxial trilinear fiber-reinforced plastic model is used for the fiber-reinforced polymer overlays.

3.1 Developing collapse fragilities from pushover

Pushover analysis is performed on a model by applying an increasing inverted triangular lateral loads pattern, representing deformation of a building under fundamental mode, and evaluating the maximum lateral displacements. Information on the structure's strength, stiffness and ductility can be extracted from the resulting capacity curve of a building, and a strength factor can be determined to evaluate the performance of a building and retrofit methods (Elkady and Lignos, 2015). Figure 4 shows the capacity curve of the reference building and the considered retrofit techniques. The capacity curve gives important information about member yielding, stiffness, and ultimate strength of a building structure. The ultimate strengths are compared with the design strength, and the strength factor is determined, which is

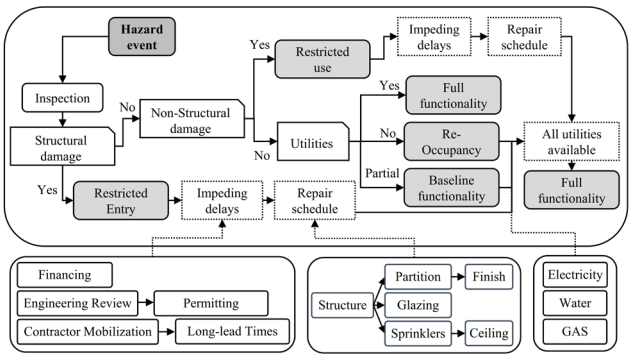

Fig. 2 Functionality states and recovery considering structural and non-structural damage, impeding delays, sequence of repairs and utility availability

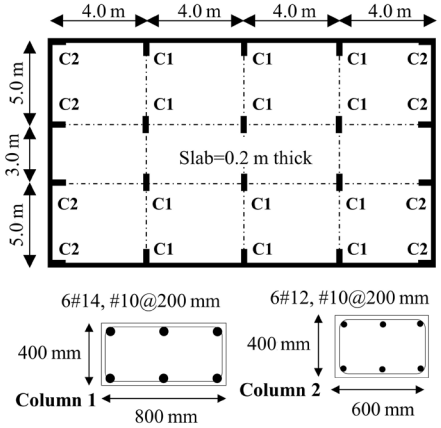

Fig. 3 Building plan and structural details

the ratio of the design strength to ultimate strength. If the strength factor is more than one, then the building is satisfactory; otherwise retrofit techniques are used to improve the strength factor. The non-ductile reinforced concrete building is designed only to resist gravity and wind loads, since before 1991 the region was classified as zone '0', and the lateral seismic loads were not considered during the design process. According to the revised zone classification of the region, static lateral force procedure provides a required design strength of 655 kN, and the ultimate strength determined from the capacity curve is 605 kN. Since the ultimate strength is less than the required design strength of a building, the reference building is not conforming to the design requirement of the current code of practice. RCJ retrofit with retrofit thickness of 50 mm, 75 mm, and 100 mm gives the strength factors of 2.69, 3.13, and 3.57. Similarly, the strength factors for the FRP retrofit for one, two and three layers are 1.54, 2.01, and 2.12, and the strength factors for the SJ retrofit with steel jacket thicknesses of 3 mm, 5 mm, and 10 mm are 2.40, 2.99 and 3.98. It is interesting to note that steel jacketing has greater impact in increasing the lateral capacity of a building, while FRPs provide comparatively the least improvement in the ultimate lateral capacity. Nonetheless, all the considered retrofit techniques provide satisfactory strength factors (i.e., greater than one).

The capacity curves are converted into idealized curves, a bilinear approximation is provided in Fig. 4(a), and more details on idealization from the capacity curve can be obtained from Elnashai and Di Sarno (2008). The four segments of the idealized curve will give four control points, which are used as an input in the SPO2IDA tool, and the median and dispersion values for the collapse fragilities are evaluated. Lognormal cumulative distribution function is then used to develop collapse fragilities for each model. Figure 5 shows the collapse fragilities developed by using pushover analysis. It is

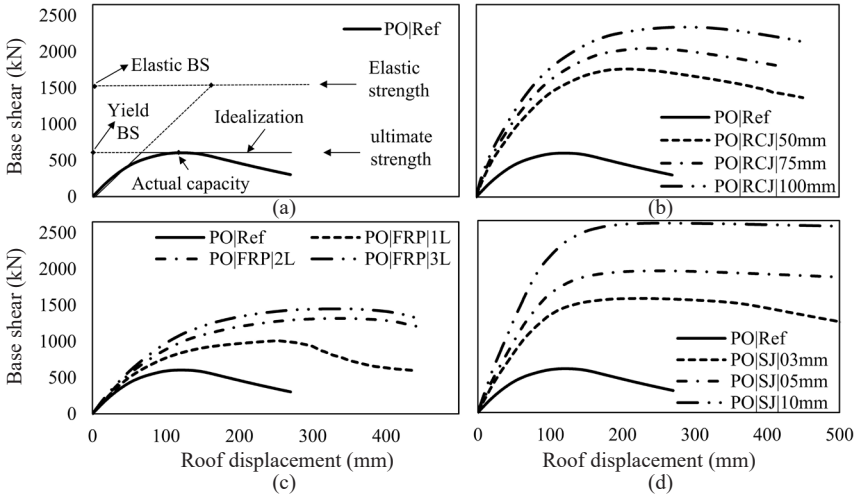

Fig. 4 Capacity curve for (a) reference structure, (b) reinforced concrete jacketing, (c) FRP overlays, and (d) steel jacketing

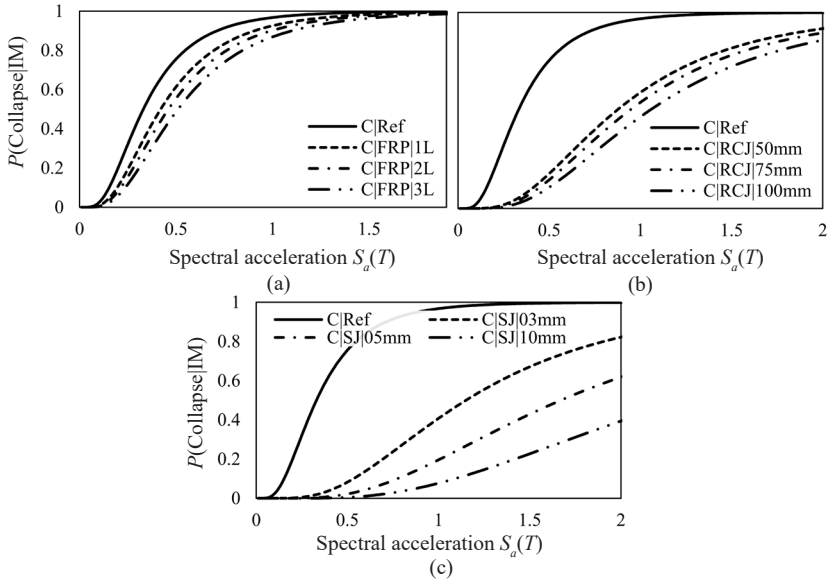

Fig. 5 Collapse fragilities for (a) FRP overlays, (b) reinforced concrete jacketing, and (c) steel jacketing

noted that SJ retrofit reduces the probability of collapse significantly, RCJ retrofit also significantly reduces the probability of collapse, while for the FRP retrofit, the reduction in the probability of collapse is not significant. Nonetheless, probability of collapse is reduced for all the considered retrofit techniques.

3.2 Consequence assessment

Consequence assessment starts with selecting a hazard scenario and assembling a building performance model. The hazard scenario with a design PGA of 0.16 g is selected for the case of this illustrative example. In order to investigate the variation of social, economic and environmental consequences with varying intensity measure, four hazard scenarios are considered for the consequence assessment (i.e., half the design hazard scenario, twice the design hazard scenario, and four times the design hazard scenario). Three retrofit techniques (i.e., FRPs with 1 layer, RCJ with 75 mm of jacket thickness, and SJ with 3 mm of jacket thickness) are considered for the consequence and resilience assessment.

The building performance model consists of fragility functions and consequence functions. Fragility functions relate the structural analysis results to the damage, and consequence functions translate the damages into social, economic, and environmental consequences. The fragility and consequence functions used in this example are extracted from (FEMA, 2012; Hashemi *et al*., 2019; Mitrani-Reiser, 2007), and are shown in Table 1. The fragility and consequence functions for various types of retrofitted structural components is not yet available in the literature. Therefore, in this illustrative example, conventional fragility and consequence functions are utilized for the retrofitted buildings.

The components are divided into drift-sensitive and acceleration-sensitive components. The components partitions, finishes, and glazing are sensitive to lateral story drifts, and ceiling and sprinklers are sensitive to floor accelerations. The social consequences are determined by constructing a population model, and defining casualty function and the population at risk. The time dependent population model represents the percentage of people present during the time of the day, and day of the week for a given realization. The casualty function for the reinforced concrete residential construction indicates that 90% will suffer fatalities in the event of collapse, and 10% will suffer a major injury in the case of reinforced concrete frame structure (FEMA, 2012). Figure 6 shows the social losses in terms of total number of expected fatalities given four scenarios. The social losses for the reference un-retrofitted building has the highest number of expected fatalities. Applying retrofit reduces the social losses, with SJ and RCJ being the most effective in reducing the social consequences.

In order to evaluate the economic and environmental losses, structural analyses of a nonlinear building models are performed and engineering demand parameters (i.e., story drifts and accelerations) are extracted for each story, correlated with damage through fragility functions and consequences through consequence functions. The total economic and environmental consequences

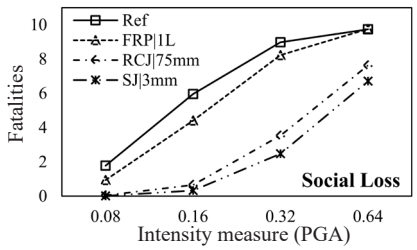

Fig. 6 Social consequence in terms of expected fatalities given IM

Table 1 Fragility functions and consequence functions of damageable components

Components	Quantity per floor	Damage state	Fragility functions		Consequence functions					
					Economic (USD)		Environmental ($kgCO_2$)		Repair time (Day)	
			Median	CoV.	Median	CoV.	Median	CoV.	Median	CoV.
Structural columns	20 units	DS_1	1.75	0.40	6270	0.39	1.794	0.4	18.9	0.46
		DS_2	2.25	0.40	9540	0.32	1.794	0.4	28.7	0.40
		DS_3	3.22	0.40	11580	0.30	19.73	0.4	35.3	0.39
Partition	6 m^2 × 22	DS_1	0.39	0.17	115	0.20	12.72	0.4	0.136	0.30
		DS_2	0.85	0.23	679	0.10	25.52	0.4	0.797	0.30
Finish	6 m^2 × 44	DS_1	0.39	0.17	115	0.20	1.336	0.4	0.135	0.51
		DS_2	0.85	0.23	321	0.10	2.686	0.4	0.376	0.61
Glazing	2.8 m^2 × 5.654	DS_1	4.00	0.36	564	0.17	96.30	0.4	0.582	0.29
		DS_2	4.60	0.36	564	0.17	183.2	0.4	0.582	0.40
Ceiling	232 m^2 × 0.22	DS_1	0.35	0.40	4541	0.40	1.023	0.4	5.699	0.63
		DS_2	0.55	0.40	37612	0.50	5.846	0.4	47.05	0.40
		DS_3	0.80	0.40	70769	0.55	19.73	0.4	88.40	0.40
Sprinklers	4 m × 8.8	DS_1	0.32	1.40	1154	0.37	58.07	0.4	1.227	0.80

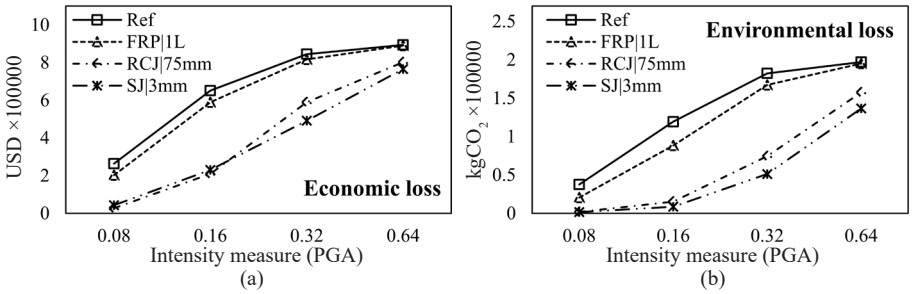

Fig. 7 Consequences (a) economic in terms of monetary loss, and (b) environmental in terms of kgCO_2 emissions

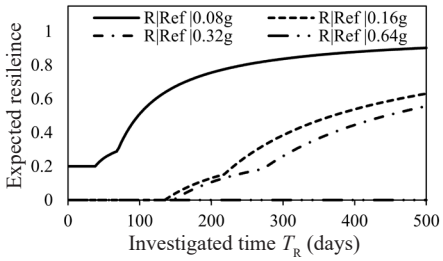

Fig. 8 Expected resilience of a reference un-retrofitted building under given scenarios

determined from Eq. (2) are shown in Fig. 7. The economic and environmental consequences increase with increasing IM levels. The un-retrofitted structure has the highest consequences, reduced using retrofit techniques. Comparatively, the percent reduction in the social, economic, and environmental consequences is highest for the 0.16 g and 0.32 g hazard scenario, and lowest for the 0.08 g and 0.64 g hazard scenario. In the given illustrative example, SJ and RCJ are more effective in reducing the consequences for the design and twice the design seismic hazard scenario.

3.3 Seismic resilience assessment

The first step in evaluating the seismic resilience is to extract the repair times for all the damageable components of a building. Table 2 shows the repair time functions given damage state, utilized to determine repair times for all the components for a given story. The next step is to develop a logical repair sequence for the downtime of a building. The building repair starts with repairing the structural components serially (i.e., structural components of the first story are repaired first, before moving to the higher stories). Not all non-structural components can be repaired simultaneously (e.g., to repair ceilings the sprinklers need to be repaired first, and in order to do finishes, partitions needed to be repaired). In the example considered, partition, glazing and sprinklers are simultaneously repaired in parallel, followed by finish and ceilings. Additional delays due to impeding factors (i.e., delays due to inspection, engineering mobilization, financing, contractor mobilization, and permitting), and utilities (i.e., water, gas, and electricity) are considered using lognormal cumulative distribution functions. The utility disruption curves represent the restoration of utilities to the building and are determined from previous earthquake data and simulation studies (Almufti and Willford, 2013). The utility disruptions depend on the amount of local damage to the distribution system and are considered through repair rate (RR), which is computed based on the peak ground velocity at a building site. The related lognormal distribution function is selected for repair rates greater or less than 0.2 repairs/km, as shown in Table 2.

In a pre-hazard state, the building is performing its intended purpose and is in full functional state (i.e., all the utilities are available and no structural or non-structural damage hinders the normal intended functions). After an earthquake event, the building can be in any of the functional states as presented in Fig. 2, depending upon the structural and non-structural damage and utility availability. The functionality state recovery times can be evaluated, and a functionality recovery curve can be generated, which gives the propagation of functional states to full functionality given the investigated time interval. The functionality curve can be utilized to develop resilience using Eq. (3). The resilience of a reference building determined for the given four scenarios is shown in Fig. 8. It is observed that for a hazard scenario with maximum PGA of 0.08 g, the building showed better resilience, but for the rest of the hazard scenarios it showed poor resilience. In the hazard scenario of 0.64, the building has negligible expected resilience even at 500 days of investigated time interval, showing that the building has collapsed and cannot be repaired.

Applying the retrofit reduces the damage, hence improving the functionality curves and seismic resilience. Figure 9 shows the functionality curves and the resulting seismic resilience of the reference building along with the retrofit techniques applied. The reference un-retrofitted building at a PGA of 0.32 g takes an expected 272.5 days to achieve full functionality, which is reduced to 260.5, 107, and 85.5 days after applying FRP, RCJ, and SJ retrofits. The improvement in seismic resilience in the case of FRP retrofit techniques is negligible, while significant improvement is observed for the RCJ, and SJ retrofit techniques. Since, seismic resilience is a function of collapse fragility, EDPs, fragility functions, and the consequence functions. It is observed that applying RCJ

Table 2 Impeding factors for delay and utility disruption curves

Impeding Factors and utility system	Mitigation measures	Damage conditions	Median	CoV.
Inspection	BORP Equivalent	-	1 day	0.54
Engineering mobilization	Engineer on contract	Minor	2 weeks	0.32
		Extensive	4 weeks	0.54
Financing	Pre-arranged credit	-	1 week	0.54
Contractor mobilization	GC on contract	Minor	3 weeks	0.66
		Extensive	7 weeks	0.35
Permitting	GC on contract	Minor	1 week	0.86
		Extensive	8 weeks	0.32
Electricity system	-	-	3 days	1.0
Water system	RR <= 0.2 repairs/km	-	4 days	0.5
	RR > 0.2 repairs/km		21 days	1.0
Natural gas system	RR <= 0.2 repairs/km	-	10 days	0.5
	RR > 0.2 repairs/km		42 days	0.6

RR = Repair rate, BORP = Building resumption program, GC = General contractor

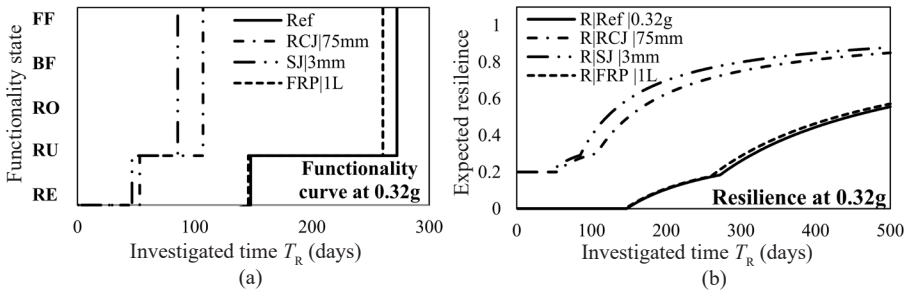

Fig. 9 Seismic hazard scenario of 0.32g showing (a) functionality curves, and (b) seismic resilience

and SJ can effectively reduce the collapse fragility and the demands on EDPs as compared to FRPs. As a result, the seismic resilience for RCJ and SJ is larger compared with the FRP retrofit alternative.

4 Conclusions

This paper presents a performance-based methodology for evaluating seismic resilience under conventional structural retrofit techniques. The social, economic, and environmental consequences are evaluated and compared for a reference un-retrofitted, and a retrofitted building. It is concluded that applying retrofit techniques reduces the probability of collapse, social, economic, and environmental consequences. The repair times of a building's components are also reduced, hence improving the seismic resilience.

The following conclusions can be drawn.

1. Pushover analysis provides important information on a structure's strength, stiffness and ductility, which can be used for preliminary evaluation of a building and the suitability of the considered retrofit technique. The strength factor determined from the capacity curve for the reference un-retrofitted building was 0.92, indicating non-conformance with the current building codes, and hence, structural modifications are required to improve the performance of a building.

2. Three retrofit techniques, namely, RCJ, SJ and FRPs, were used for improving the performance of a deficient building. Capacity curves for the retrofit buildings showed improved strength factors, hence improving the overall seismic performance of a building. The SJ retrofit technique significantly improved the performance of a building, followed by the RCJ retrofit. The FRPs also improved the performance above the acceptable code performance, but comparatively the performance improvement was not significant.

3. The social, economic, and environmental consequences for the reference and retrofit buildings were assessed in term of casualties, monetary loss in USD, and equivalent carbon emissions. The consequences were reduced significantly by applying SJ jacketing, followed by the RCJ. In the case of FRP retrofit, the reduction in consequences were not significant.

4. The seismic resilience assessment considers component-level repair time of a building considering sequence of repairs, utility repair times, and impeding delays for the downtime assessment of a building. Five discrete functionality states were considered for developing the functionality repair curve to evaluate seismic resilience. Among the considered retrofit alternatives, SJ and RCJ showed better seismic resilience,

while FRPs and the un-retrofitted building showed poor seismic resilience.

Acknowledgement

The first author acknowledge funding provided by the Research Grants Council (RGC) of Hong Kong under the Hong Kong PhD Fellowship Scheme (HKPFS) of 2018. This study has been supported by the Chinese National Engineering Research Centre (CNERC) for Steel Construction (Hong Kong Branch) at the Hong Kong Polytechnic University (Project No. P0013864; Programme Code: BBV9).

References

Almufti I and Willford M (2013), *REDi™ Rating System: Resilience Based Earthquake Design Initiative for the Next Generation of Buildings*, Version 1.0, October, Arup.

Anelli A, Santa-Cruz S, Vona M, *et al*. (2019), "A Proactive and Resilient Seismic Risk Mitigation Strategy for Existing School Buildings," *Structure and Infrastructure Engineering*, **15**(2): 137–151.

Anwar GA, Dong Y and Zhai C (2020), "Performance-Based Probabilistic Framework for Seismic Risk, Resilience, and Sustainability Assessment of Reinforced Concrete Structures," *Advances in Structural Engineering*, **23**(7): 1454–1472.

Asadi E, Salman AM and Li Y (2019), "Multi-Criteria Decision-Making for Seismic Resilience and Sustainability Assessment of Diagrid Buildings," *Engineering Structures*, **191**: 229–246.

ASCE-41-13 (2013), *Seismic Evaluation and Retrofit of Existing Buildings*, American Society of Civil Engineers, Reston, Virginia.

Beavers JE (2002), "A Review of Seismic Hazard Description in US Design Codes and Procedures," *Progress in Structural Engineering and Materials*, **4**(1): 46–63.

Billah AM and Alam MS (2014), "Seismic Performance Evaluation of Multi-Column Bridge Bents Retrofitted with Different Alternatives Using Incremental Dynamic Analysis," *Engineering Structures*, **62**: 105–117.

Bocchini P, Frangopol DM, Ummenhofer T, *et al*. (2013), "Resilience and Sustainability of Civil Infrastructure: Toward a Unified Approach," *Journal of Infrastructure Systems*, **20**(2).

Calvi G (2013), "Choices and Criteria for Seismic Strengthening," *Journal of Earthquake Engineering*, **17**(6): 769–802.

Cimellaro GP, Reinhorn AM and Bruneau M (2010), "Framework for Analytical Quantification of Disaster Resilience," *Engineering Structures*, **32**(11): 3639–3649.

Dong Y and Frangopol DM (2015), "Risk and Resilience Assessment of Bridges under Mainshock and Aftershocks Incorporating Uncertainties," *Engineering Structures*, **83**: 198–208.

Dong Y and Frangopol DM (2016), "Performance-Based Seismic Assessment of Conventional and Base-Isolated Steel Buildings Including Environmental Impact and Resilience," *Earthquake Engineering Structural Dynamics*, **45**(5): 739–756.

Dong Y, Frangopol DM and Saydam D (2014), "Pre-Earthquake Multi-Objective Probabilistic Retrofit Optimization of Bridge Networks Based on Sustainability," *Journal of Bridge Engineering*, **19**(6): 04014018.

Dong Y, Frangopol DM and Sabatino S (2016), "A Decision Support System for Mission-Based Ship Routing Considering Multiple Performance Criteria," *Reliability Engineering & System Safety*, **150**: 190–201.

Elkady A and Lignos DG (2015), "Effect of Gravity Framing on the Overstrength and Collapse Capacity of Steel Frame Buildings with Perimeter Special Moment Frames," *Earthquake Engineering and Structural Dynamics*, **44**(8): 1289–1307.

Elnashai AS and Di Sarno L (2008), *Fundamentals of earthquake engineering*, Wiley Online Library.

FEMA-547 (2006), *Techniques for the Seismic Rehabilitation of Existing Buildings*, Building Seismic Safety Council for the Federal Emergency Management Agency.

FEMA (2012), *Seismic Performance Assessment of Buildings: Vol. 1–Methodology*, Report Number FEMA P-58-1, Applied Technology Council for the Federal Emergency Management Agency, Washington, D.C.

Gautam D and Chaulagain H (2016), "Structural Performance and Associated Lessons to be Learned from World Earthquakes in Nepal After 25 April 2015 (M_W 7.8) Gorkha Earthquake," *Engineering Failure Analysis*, **68**: 222–243.

Giouvanidis AI and Dong Y (2020), "Seismic Loss and Resilience Assessment of Single-Column Rocking Bridges," *Bulletin of Earthquake Engineering*, DOI: 10.1007/s10518-020-00865-5.

Guo T, Xu Z, Song L, *et al*. (2017), "Seismic Resilience Upgrade of RC Frame Building Using Self-Centering Concrete Walls with Distributed Friction Devices," *Journal of Structural Engineering*, **143**(12): 04017160.

Hashemi MJ, Al-Attraqchi AY, Kalfat R, *et al*. (2019), "Linking Seismic Resilience into Sustainability Assessment of Limited-Ductility RC Buildings," *Engineering Structures*, **188**: 121–136.

Jeong S-H and Elnashai AS (2005), "Analytical Assessment of an Irregular RC Frame for Full-Scale 3D Pseudo-Dynamic Testing part I: Analytical Model Verification," *Journal of Earthquake Engineering*, **9**(01): 95–128.

Khanmohammadi S, Farahmand H and Kashani H

(2018), "A System Dynamics Approach to the Seismic Resilience Enhancement of Hospitals," *International Journal of Disaster Risk Reduction*, **31**: 220–233.

Kilanitis I and Sextos A (2019), "Integrated Seismic Risk and Resilience Assessment of Roadway Networks in Earthquake Prone Areas," *Bulletin of Earthquake Engineering*, **17**(1): 181–210.

Li Y, Dong Y, Frangopol DM, *et al*. (2020a), "Long-Term Resilience and Loss Assessment of Highway Bridges Under Multiple Natural Hazards," *Structure and Infrastructure Engineering*, 1–16, DOI: 10.1080/15732479.2019.1699936.

Li Y, Dong Y and Qian J (2020b), "Higher-Order Analysis of Probabilistic Long-Term Loss under Nonstationary Hazards," *Reliability Engineering & System Safety*, 107092.

Ma C-K, Apandi NM, Sofrie CSY, *et al*. (2017), "Repair and Rehabilitation of Concrete Structures Using Confinement: A Review," *Construction and Building Materials*, **133**: 502–515.

Mitrani-Reiser J (2007), *An Ounce of Prevention: Probabilistic Loss Estimation for Performance-Based Earthquake Engineering*, California Institute of Technology.

Molina Hutt C, Almufti I, Willford M, *et al*. (2016), "Seismic Loss and Downtime Assessment of Existing Tall Steel-Framed Buildings and Strategies for Increased Resilience," *Journal of Structural Engineering*, **142**(8): C4015005.

Mwafy A and Elkholy S (2017), "Performance Assessment and Prioritization of Mitigation Approaches for Pre-Seismic Code Structures," *Advances in Structural Engineering*, **20**(6): 917–939.

Pekcan G, Itani AM and Linke C (2014), "Enhancing Seismic Resilience Using Truss Girder Frame Systems with Supplemental Devices," *Journal of Constructional Steel Research*, **94**: 23–32.

Qian J and Dong Y (2020), "Multi-Criteria Decision Making for Seismic Intensity Measure Selection Considering Uncertainty," *Earthquake Engineering and Structural Dynamics*.

Rodriguez-Nikl T (2015), "Linking Disaster Resilience and Sustainability," *Civil Engineering and Environmental Systems*, **32**(1-2): 157–169.

Rousakis TC (2018), "Inherent Seismic Resilience of RC Columns Externally Confined with Nonbonded Composite Ropes," *Composites Part B: Engineering*, **135**: 142–148.

Su L, Wan H-P, Dong Y, *et al*. (2019), "Seismic Fragility Assessment of Large-Scale Pile-Supported Wharf Structures Considering Soil-Pile Interaction," *Engineering Structures*, **186**: 270–281.

Thermou G and Elnashai AS (2006), "Seismic Retrofit Schemes for RC Structures and Local-Global Consequences," *Progress in Structural Engineering and Materials*, **8**(1): 1–15.

Tirca L, Serban O, Lin L, *et al*. (2016), "Improving the Seismic Resilience of Existing Braced-Frame Office Buildings," *Journal of Structural Engineering*, **142**(8): C4015003.

Vamvatsikos D and Allin Cornell C (2006), "Direct Estimation of the Seismic Demand and Capacity of Oscillators with Multi-Linear Static Pushovers Through IDA," *Earthquake Engineering and Structural Dynamics*, **35**(9): 1097–1117.

Vona M, Mastroberti M, Mitidieri L, *et al*. (2018), "New Resilience Model of Communities Based on Numerical Evaluation and Observed Post Seismic Reconstruction Process, *International Journal of Disaster Risk Reduction*, **28**: 602–609.

Wang Z, Jin W, Dong Y and Frangopol DM (2018), "Hierarchical Life-Cycle Design of Reinforced Concrete Structures Incorporating Durability, Economic Efficiency and Green Objectives," *Engineering Structures*, **157**: 119–131.

Whitman RV, Anagnos T, Kircher CA, *et al*. (1997), "Development of a National Earthquake Loss Estimation Methodology," *Earthquake Spectra*, **13**(4): 643–661.

Zheng Y, Dong Y, Chen B, *et al*. (2019), "Seismic Damage Mitigation of Bridges with Self-Adaptive SMA-Cable-Based Bearings," *Smart Structures and Systems*, **24**(1): 127–139.

Zheng Y, Dong Y and Li Y (2018), "Resilience and Life-Cycle Performance of Smart Bridges with Shape Memory Alloy (SMA)-Cable-Based Bearings," *Construction and Building Materials*, **158**: 389–400.